JOURNAL OF VIROLOGY, Jan. 2009, p. 712–721 Vol. 83, No. 2
0022-538X/09/$08.00+0 doi:10.1128/JVI.01933-08

Protease-Mediated Entry via the Endosome of Human Coronavirus 229E▽

Miyuki Kawase, Kazuya Shirato, Shutoku Matsuyama, and Fumihiro Taguchi*

Laboratory of Respiratory Viral Infections, Department of Virology III, National Institute of Infectious Diseases, Musashi-Murayama, 208-0011 Tokyo, Japan

Received 15 September 2008/Accepted 21 October 2008

Human coronavirus 229E, classified as a group I coronavirus, utilizes human aminopeptidase N (APN) as a receptor; however, its entry mechanism has not yet been fully elucidated. We found that HeLa cells infected with 229E via APN formed syncytia when treated with trypsin or other proteases but not in a low-pH environment, a finding consistent with syncytium formation by severe acute respiratory syndrome coronavirus (SARS-CoV). In addition, trypsin induced cleavage of the 229E S protein. By using infectious viruses and pseudotyped viruses bearing the 229E S protein, we found that its infection was profoundly blocked by lysosomotropic agents as well as by protease inhibitors that also prevented infection with SARS-CoV but not that caused by murine coronavirus mouse hepatitis virus strain JHMV, which enters cells directly from the cell surface. We found that cathepsin L (CPL) inhibitors blocked 229E infection the most remarkably among a variety of protease inhibitors tested. Furthermore, 229E infection was inhibited in CPL knockdown cells by small interfering RNA, compared with what was seen for a normal counterpart producing CPL. However, its inhibition was not so remarkable as that found with SARS-CoV infection, which seems to indicate that while CPL is involved in the fusogenic activation of 229E S protein in endosomal infection, not-yet-identified proteases could also play a part in that activity. We also found 229E virion S protein to be cleaved by CPL. Furthermore, as with SARS-CoV, 229E entered cells directly from the cell surface when cell-attached viruses were treated with trypsin. These findings suggest that 229E takes an endosomal pathway for cell entry and that proteases like CPL are involved in this mode of entry.

Human coronavirus 299E (HCoV 229E), a causative agent of the human common cold (44), is classified as a group I coronavirus and is an enveloped virus having RNA consisting of a single, positive-stranded genome of about 30 kb (21). Human aminopeptidase N (APN), a surface metalloprotease found on the apical membranes of a variety of cells, serves as a receptor for HCoV 229E (17, 49).

Spike (S) protein of HCoV 229E, categorized as a class I fusion protein, is responsible for the binding to APN and entry into cells (3, 6). Although the S protein of group II coronavirus mouse hepatitis virus (MHV) is cleaved by a host-cell-derived protease into two subunits, namely, N-terminal S1 and C-terminal S2, during biogenesis in the exocytic pathway (35), 229E S is not cleaved in cells and S protein on the virion is an uncleaved form (6). However, the 229E S protein consists of two regions corresponding to S1 and S2 of the cleaved subunits of MHV. The former is responsible for receptor binding and the latter for entry. The receptor-binding site of 229E S encompasses the internal region of S1, consisting of amino acids 417 to 547 (3, 41), and differs from the location of the MHV receptor-binding site, which is in the N-terminal 330 amino acids of the S1 subunit (19, 36). S1 proteins vary among different coronaviruses; even in a given coronavirus group, S1 proteins are highly divergent (6). However, the S2 or S2-corresponding regions of coronaviruses share common structural and biological features (5, 6, 9). These observations suggest a common entry mechanism utilized by various coronaviruses.

Enveloped viruses enter cells through the fusion of their envelope with the plasma membrane or endosomal membrane. Human immunodeficiency virus (HIV) enters cells via a plasma membrane (7, 12, 45). The binding to the receptor/coreceptor induces conformational changes together with the fusion activation of gp160 of HIV, which, in turn, facilitates fusion of the viral envelope and plasma membrane (7, 12). This mechanism is utilized by a number of retroviruses, paramyxoviruses, and coronaviruses (12, 45). In contrast, the influenza virus prototypically utilizes an endosomal pathway for entry. Its hemagglutinin protein is not activated by binding to its receptor but rather is activated for fusion in the acidic environment of the endosome (low-pH-dependent entry). A similar mode of entry is used by vesicular stomatitis virus (VSV) and others as well (45). A third mode of entry was reported as a mechanism for Ebola virus that enters cells via an endosomal compartment, and acidic condition in the endosomes is critical for entry (8, 39, 47). However, it is not the acidic conditions but rather proteases that trigger conformational changes and fusion activation of GP protein (protease-dependent entry) (8). Severe acute respiratory syndrome coronavirus (SARS-CoV) has been also reported to enter cells in a protease-dependent fashion as well (33, 34).

Cells infected with nonfusogenic coronaviruses, such as SARS-CoV or MHV-2, form syncytia after trypsin treatment (26, 30, 34, 50). Syncytium formation was also observed in the presence of trypsin in cells infected with porcine epidemic diarrhea virus or bovine coronavirus (20, 40). The 229E-infected cells also formed syncytia in the presence of some trypsin-like proteases and the infection was inhibited by cysteine

* Corresponding author. Mailing address: Laboratory of Viral Respiratory Infections, Department of Virology III, National Institute of Infectious Diseases, Musashi-Murayama, 208-0011 Tokyo, Japan. Phone: 81-42-561-0771, ext. 3533. Fax: 81-42-567-5631. E-mail: ftaguchi@nih.go.jp.

▽ Published ahead of print on 29 October 2008.

and the trypsin-like protease inhibitor leupeptin (2). These features of 229E are shared by SARS-CoV (26, 34), which suggests the possibility that 229E enters into cells in a fashion similar to that of SARS-CoV. In the present study, we have tested this possibility by using HeLa cells permissive to 229E infection. Our results suggest that 229E enters cells via endosomes in which proteases active in a low-pH environment, most likely cathepsin L (CPL) and other proteases, are involved in the fusogenic activation of 229E S protein, leading us to conclude that the 229E cell entry mechanism is similar to that of SARS-CoV.

MATERIALS AND METHODS

Cells. HeLa cells maintained in our institute, expressing human APN and permissive to 229E infection, were transformed to express the receptor for SARS-CoV, human angiotensin-converting enzyme 2 (ACE2) (23), as well as the MHV receptor, carcinoembryonic antigen-related cell adhesion molecule 1 (CEACAM1) (10, 11, 46). HeLa cells expressing ACE2 were established by transfecting the expression plasmid for ACE2 and through selection in a medium containing G418 as described previously (51). The cell line that showed high sensitivity to SARS-CoV (designated HeLa-A cells) was further transfected with an expression plasmid containing the CEACAM1 gene (24, 31) and selected in a medium containing blastocidin. The cell line sensitive to 229E, SARS-CoV, and MHV and expressing ACE2 and CEACAM1 (HeLa-AC), was selected. Those cells were grown and maintained in Dulbecco's modified minimal essential medium (DMEM; Nissui, Tokyo, Japan) containing 5% and 1% fetal bovine serum (Sigma, St Louis, MO) as growth medium (GM) and maintenance medium (MM), respectively. All of the HeLa, HeLa-A, and HeLa-AC cell lines we isolated proved to be sensitive to VSV infection as well.

Virus and virus infection. HCoV 229E was kindly provided by R. Nomura (28) and initially grown in L132 cells, a subline of HeLa cells. The viruses were then grown in HeLa cells. For the propagation of 229E as a seed virus, viruses were inoculated onto HeLa cells with a multiplicity of infection (MOI) of 0.5 to 1 and adsorbed at 34 C for 1 h. Then, cells were cultured with MM at 34°C for 2 days. Culture supernatants as well as infected cells were used after ultrasonication as described previously (27). Viruses divided into a small volume were stored at −80°C until use. MHV-2 and MHV-JHMV sp-4 also used in this experiment were prepared as described elsewhere (38, 48). Pseudotyped VSV that expresses green fluorescent protein (GFP) and harbors SARS-CoV S protein or VSV G protein was prepared as described previously (15). The production of a VSV pseudotype bearing 229E S protein is described below.

Plaque assay. Plaque assay of HCoV 2.29 E was done using HeLa cells prepared in 24-well plates with a modified plaque assay for MHV as described previously (37). Confluent HeLa cells in 24-well plates (Falcon, Lincoln Park, NJ) were inoculated with 50 μl of 10-fold serially diluted virus samples and incubated at 34°C for 40 to 50 min. Then, cells were overlaid with 0.5 ml of MM containing 1% carboxylmethyl cellulose (Wako, Tokyo, Japan) at 34°C for 2 days. Cells were then washed once with phosphate-buffered saline (PBS), pH 7.2, and treated with 200 μg/ml of trypsin at room temperature (RT) for 5 min. After the removal of trypsin, cells were further incubated at 34°C for 2 to 3 h in MM, until syncytia were visible. Alternatively, infected cells were cultured with DMEM plus 10% tryptose phosphate broth (TPB; Difco, Detroit, MI) plus 1% carboxylmethyl cellulose containing 5 μg/ml of trypsin for 24 h. Cells were then fixed with formalin and stained with crystal violet. Plaques of syncytia were counted by use of light microscopy.

Blockade of 229E infection by anti-APN antibodies. HeLa cells cultured in GM in a 96-well plate (Smilon, Tokyo, Japan) were treated with serially diluted anti-APN antibody WM15 (Biolegend, San Diego, CA) at 4°C for 45 min. Then, cells were infected with ca. 150 PFU of 229E, incubated at 4°C for 45 min, and further incubated at 34°C in GM for 20 to 24 h in the presence of anti-APN antibody. After fixing with cold ethanol-acetone (1:1) for 5 min, infected cells were examined for 229E antigen with anti-229E antibodies raised using rabbit and fluorescein isothiocyanate-labeled anti-rabbit serum. Antigen-positive cells were counted by use of fluorescence microscopy. The inhibition of infection by the antibody was calculated in comparison with the antigen-positive cell number obtained without treatment of APN antiserum.

Generation of VSV pseudotyped with 229E S protein. To generate VSV pseudotyped with 229E S protein, we first of all isolated the cDNA for the 229E S protein with a 19-amino-acid truncation from the C terminus. The S protein with a 19-amino-acid deletion was reported to be efficiently incorporated into VSV pseudotyped virus (15). The gene encoding this protein was amplified by a reverse transcription-PCR with a specific primer set (the sense primer was 5′-CCGCTCGAGGCCGCCACCATGTTTGTTTTGCTTGTTGCATATGCC-3′, and the antisense primer was 5′-CGGGGTACCTCATCTAATAGAAGATGCAAAACAACTAAAG-3′; underlining indicates the recognition sites of XhoI and KpnI) and then cloned into the XhoI-KpnI site of the mammalian expression vector pTarget (Promega, Madison, WI). The sequence of the constructed plasmid was confirmed using the BigDye Terminator cycle sequencing kit version 3.1 and the ABI Prism 3130xl genetic analyzer (Applied Biosystems, Foster City, CA), and the plasmid was designated as pTarget 229ES-del19. The 293T/17 cells obtained from the American Tissue Culture Collection (ATCC) (catalog no. CRL-11268) were transfected with the above-described expression plasmid by use of TransIT-293 transfection reagent (Mirus Bio, Madison, WI) and incubated at 34°C for 40 h. Those cells were then infected with VSVΔG*-G, in which the VSV G gene is replaced by a GFP gene and a VSV G protein is harbored (kindly provided by M. A. Whitt, GTx, Inc., Tennessee) and incubated at 34°C for 1 h. After four washes with PBS, those cells were further incubated at 34°C for 24 h. The culture fluid was collected, centrifuged at 1,000 rpm for 5 min at 4°C, divided into small volumes, and stored at −80°C until use. As controls, VSV pseudotyped viruses bearing SARS-CoV S and VSV G proteins were generated in the same way as reported previously (15). The infectivities of those pseudotyped viruses were determined by reference to the number of GFP-positive cells and are shown as infectious units (IU).

Proteases. The proteases used in this study are trypsin (T-8802; Sigma), thermolysin (P1512; Sigma), chymotrypsin (C-3142; Sigma), dispase (1 276 921; Roche, Branchburg, NJ), papain (53J6521; Worthington Biochemicals, Freehold, NJ), proteinase K (Wako, Tokyo, Japan), collagenase (C-5183; Sigma), and elastase (E-0258; Sigma). These proteases were dissolved in PBS and used at the indicated concentrations in PBS. Cells infected with 229E cultured in MM were washed once with PBS and treated with various concentrations of proteases at RT for 5 min. Then, proteases were removed and cells were further incubated in MM for 2 to 3 h until the syncytia became detectable under light microscopy.

Treatment of virions with proteases. To see whether trypsin induced cleavage of 229E S protein, we used concentrated virions. 229E in culture fluid consisting of DMEM plus 10% TPB was clarified by centrifugation at 5,000 rpm for 20 min, and the supernatants were concentrated ca. 10-fold by ultrafiltration (Amicon Ultra, Ultracel-100K; Millipore, Massachusetts). These virions were treated with trypsin at different concentrations at RT for 5 min and then analyzed by Western blotting after sodium dodecyl sulfate-polyacrylamide gel electrophoresis (SDS-PAGE) as described previously (24). HeLa cells infected with 229E at an MOI of 1 were treated with trypsin at 1 day postinfection at RT for 5 min and the proteins were analyzed by Western blotting after SDS-PAGE. Virions were also treated with 36 μg/ml of CPL (219402; Calbiochem) or 36 μg/ml of cathepsin B (CPB) (219362; Calbiochem) in a buffer containing 130 mM NaCl, 40 mM HEPES, pH 5.0 and 40 mM MES (morpholineethanesulfonic acid), pH 5.0 at 37°C for 30 min. Then, the resultant virions were analyzed by Western blotting with anti-S2 antibody.

Treatment of cells with lysosomotropic agents and protease inhibitors. To see the effect of bafilomycin (Baf; Sigma) and ammonium chloride (NH_4Cl) (Wako), that blocks the acidification of the endosome, we used infectious viruses or pseudotyped VSV bearing 229E S, SARS-CoV S, or VSV G protein. HeLa-AC cells in 24-well plates were treated with Baf (1 μM) or NH_4Cl (50 mM) in MM for 1 h at 37°C and were infected with 5×10^5 PFU of 229E, MHV-JHM, or MHV-2. After incubation for 1 h at 34°C (229E) or 37°C (MHVs) in the presence of those agents, cells were washed once with PBS and fed in MM in the presence of agents for 3 h. Then, the medium was changed to MM without agents. At 24 or 10 h after infection with 229E or MHVs, respectively, virus titers in cells were examined by a plaque assay. Unless otherwise stated, the adsorption and incubation of infected cells were carried out at 34°C and 37°C for 229E and MHVs, respectively. In some experiments, HeLa cells in 24-well plates were treated with 500 nM Baf in MM from 1 h before to 4 h after 229E infection or from 4 to 24 h after infection with 5×10^5 PFU of 229E, and virus titers were examined at 24 h.

In the analysis using VSV pseudotype, HeLa-A cells prepared in 96-well plates were treated with different concentrations of Baf for 60 min. After removing Baf, we infected the cells with pseudotyped viruses of approximately 500 IU in 50 μl of medium containing Baf and incubated at 37°C for 1 h for adsorption. After washing cells with PBS, we incubated them for a further 24 h in the presence of Baf. GFP-positive cells were photographed under a Keyence fluorescence microscope (Keyence Corporation, Osaka, Japan) and counted by using image measurement and analysis software VH-H1A5, version 2.6 (Keyence). The inhibitory effect of the Baf was calculated by dividing GFP-positive cell numbers in treated cells by the number obtained from untreated cells. NH_4Cl was also used in a manner similar to that employed with Baf.

Cells were also treated with a variety of protease inhibitors to determine the

involvement of protease in the entry process of 229E by using VSV pseudotypes bearing either 229E S protein, SARS-CoV S protein, or VSV G protein. The protease inhibitors used were as follows: cysteine protease and trypsin-like protease inhibitor leupeptin (Roche), CPL inhibitor EST (Calbiochem), MDL28107 (Sigma), CPB inhibitor CA-074 (Sigma), cathepsin K (CPK) inhibitor II (Z-L-NHNHCONHNH-LF-Boc; Calbiochem), cathepsin S (CPS) inhibitor (Z-FL-Cocho; Calbiochem), and CPL inhibitor II (Z-FY-Cho; Calbiochem). Cells were treated with these protease inhibitors in a manner similar to the treatment with Baf, and their effect on infection by pseudotypes with 229E S, SARS-CoV S, and VSV G proteins was determined by the quantification of GFP-positive cells as described above.

Knockdown of CPL by siRNA. Small interfering RNA (siRNA) oligonucleotides targeting CPL (L-005841-00-005) and control nontargeting siRNA (D-001810-10-05) were purchased from Dharmacon (Chicago, IL). HeLa-A cells were treated with those siRNAs according to the manufacturer's recommendation. Briefly, 50%-subconfluent cells prepared 1 day before use in 96-well plates were incubated with GM containing 100 nM of siRNA for 3 to 4 days. Then, those cells were infected with pseudotyped VSV bearing 229E S, VSV G, or SARS-CoV S protein. The GFP-positive cells were counted 24 h later under a Keyence fluorescence microscope, and the percentage of inhibition was obtained by comparing the values for GFP-positive cells treated with control nontargeting siRNA.

Potentiation of 229E infection from cell surface. 229E was facilitated to infect from the cell surface, as described previously for the cell surface infection with SARS-CoV (26, 42). HeLa-A cells were treated with 500 nM Baf for 60 min at 37°C to block the endosomal pathway, and then cells were kept on ice. Those cells were infected with pseudotyped VSV bearing the 229E S protein on ice for 30 min and then treated with 100 μg/ml trypsin at RT for 5 min. Cells were further incubated at 37°C for 24 h in the presence of 500 nM Baf. Virus infection was estimated by the expression of GFP as described previously (15). VSV pseudotypes bearing SARS-CoV S protein or VSV G protein were also used as controls.

Western blotting. Samples for Western blot analysis were lysed in a lysis buffer and subjected to SDS-PAGE as described previously (25). The proteins in the gel were transferred onto a polyvinylidine difluoride membrane (25), and S protein was detected with anti-S2 antibodies raised with a synthetic peptide derived from the C-terminal region of the S protein in rabbits, kindly provided by R. Nomura. Western blot analysis of CPL was done with anti-Cat-L (Athens Research and Technology, Athens, GA). Then, the bands were visualized using Supersignal West Dura (Pierce, Rockford, IL) with LAS-1000PLUS (Fujifilm, Tokyo, Japan).

RESULTS

Syncytium formation of 229E-infected HeLa cells after treatment with proteases. Cell lines permissive to HCoV 229E infection are restricted. L132 or MCR-5 cells have been generally used for infectious assays of 229E (28, 41). L132 is a subclone derived from HeLa cells, although these two cell lines are morphologically distinct. We have examined whether the HeLa cells maintained in our institute were permissive to 229E infection or not. When HeLa cells were infected with 229E and cultured for 2 days, there appeared to be no cytopathic changes (Fig. 1A). However, 229E-inoculated cells were found to be antigen positive when examined by indirect immunofluorescence using anti-229E antibodies (Fig. 1A), which indicated that the HeLa cells we used are permissive to 229E infection. Since cells infected with other coronaviruses without inducing syncytium formation, such as SARS-CoV and MHV-2, developed syncytia following trypsin treatment (26, 34, 50), we examined the effect of trypsin on 229E-infected cells. As shown in Fig. 1A and B, cells infected with 229E formed syncytia with 229E antigens after treatment with trypsin. These results showed that our HeLa cells were susceptible for 229E infection, and infected cells developed syncytia when treated with trypsin. However, cells infected with 229E treated with a buffer of pH 5.0 did not exhibit syncytium formation (Fig. 1B). These features of 229E are similar to those of SARS-CoV and MHV-2.

We have also examined the effects of a variety of proteases on the fusion formation of 229E-infected HeLa cells. Infected cells were treated with proteases at the highest concentration that does not give overt effects in noninfected HeLa cells. As shown in Fig. 1C, a variety of proteases, such as proteinase K and thermolysin, induced large syncytia as efficiently as trypsin did, while elastase, dispase, chymotrypsin, and papain induced syncytia slightly or apparently smaller than the syncytia induced by trypsin treatment. Collagenase treatment failed to induce syncytia. The findings of syncytium formation by those proteases and the failure of collagenase to induce syncytia on 229E-infected cells were quite similar to those relative to syncytium formation by SARS-CoV, as described previously (26).

Cleavage of the S protein by trypsin. We have examined, by using 229E virions, whether syncytium formation is attributed to S protein cleavage, as reported for SARS-CoV and MHV-2 (26, 30). 229E virions concentrated by ultrafiltration as described in Materials and Methods were treated with varied concentrations of trypsin at RT for 5 min, and the S protein was analyzed by Western blotting using anti-229E S antibodies. 229E-infected or mock-infected cells were also treated with trypsin and analyzed by Western blotting. As shown in Fig. 2, the virions without trypsin treatment contained a protein of ca. 200 kDa, a finding which suggested that this protein corresponds to uncleaved 229E S. Likewise, in 229E-infected cells untreated with trypsin, only a 200-kDa band was detected. After treatment with trypsin, two other bands, one of 80 to 85 kDa and the other of ca. 150 kDa, became visible for the virions as well as for the infected cells. The smaller band was always found after treatment with trypsin, although a band of ca. 150 kDa was not seen in some cases, especially when virions were treated with low concentrations of trypsin (data not shown). Since the antibody used for this analysis is against the C-terminal region of S, the 80- to 85-kDa protein seems to correspond to the S2 subunit of MHV, while a 150-kDa protein would result from the cleavage at the site further upstream from the cleavage site producing the 80- to 85-kDa protein. A 150-kDa protein would not be involved in the fusion formation, since this band was not always found in cell lysates after treatment by trypsin, even when cell-to-cell fusion was induced. There may be a site in the S protein highly sensitive to trypsin treatment, which would result in the production of a 150-kDa fragment.

APN expressed on HeLa cells and utilized as a receptor for 229E. Since it was revealed that trypsin treatment induced syncytium formation in 229E-infected cells, we have established a plaque assay as described in Materials and Methods. As shown in Fig. 3A, plaques consisting of fused cells were produced 1 to 2 days after infection in the presence of trypsin. The plaque assay showed the one-hit kinetics, as shown in Fig. 3B, indicating that a plaque is produced by an infectious virus; this plaque assay is highly reliable for infectivity testing. Since 229E is known to utilize human APN as a receptor for infection (17, 49), we have examined whether the infection of HeLa cells is mediated by the APN. The infection with 229E was blocked by anti-APN antibody in a concentration-dependent manner (Fig. 3C) and not blocked by control antibody (data not shown), indicating that our HeLa cells are infected via APN and that no alternative receptor is used for the infection.

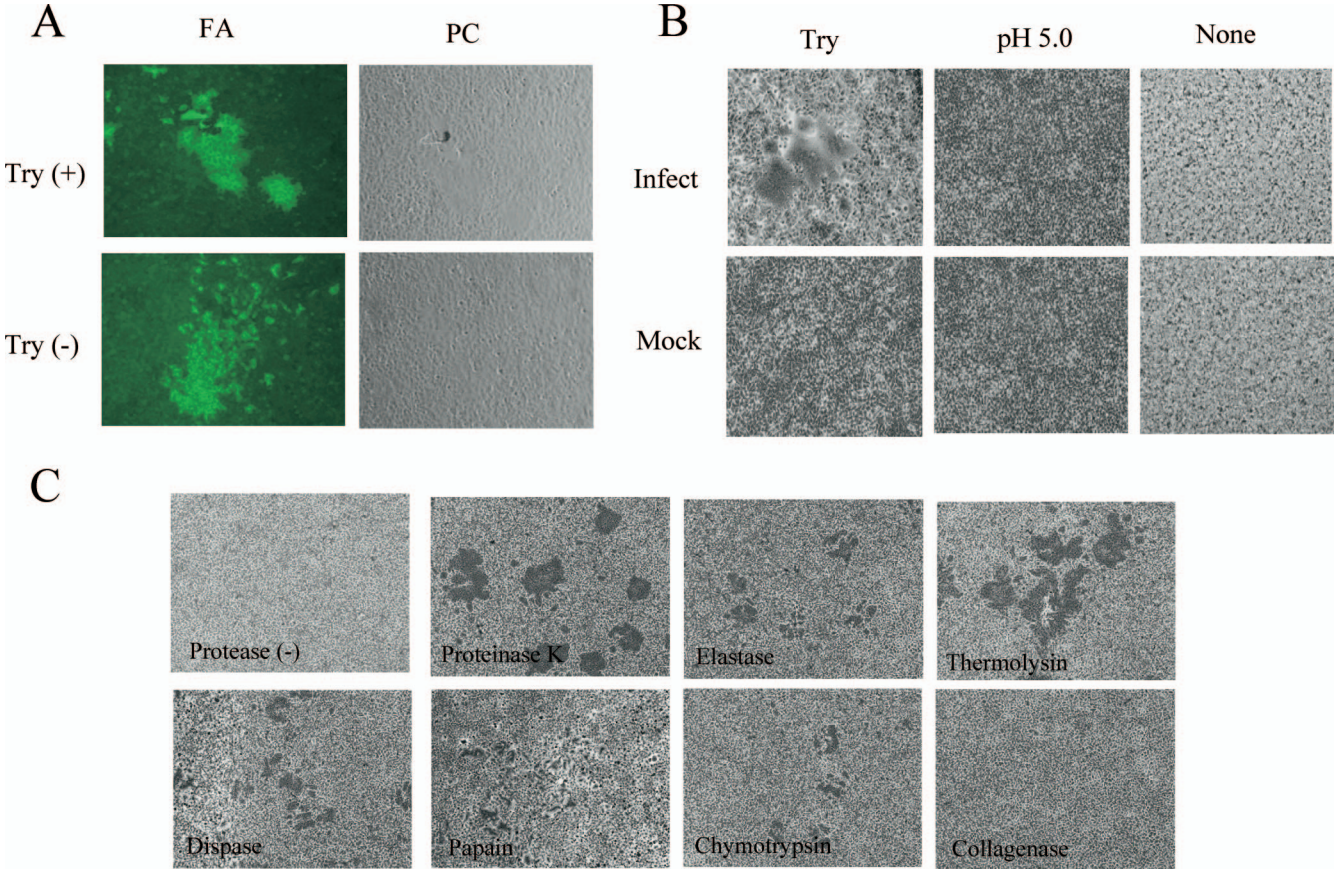

FIG. 1. Syncytium formation of 229E-infected HeLa cells induced by trypsin and other protease treatment. (A) HeLa cells infected with 229E were cultured for 2 days and then treated or left untreated with trypsin (Try; 100 μg/ml) at RT for 5 min. Cells were cultured for an additional 2 h and observed for syncytium formation and viral antigen via phase-contrast (PC) and fluorescent (FA) microscopy, respectively. (B) Cells infected (Infect) with 229E or mock infected (Mock) were cultured for 2 days and treated with 100 μg/ml of trypsin (Try) or DMEM adjusted to pH 5.0 at RT for 5 min. After 2 h of culture, cells were fixed with formaldehyde and stained with crystal violet. Cells without any treatment were shown as controls (None). (C) Syncytium formation of cells infected with 229E was induced by treatment with various proteases. HeLa cells infected with 229E and cultured for 2 days were treated with a variety of proteases at RT for 5 min and cultured for an additional 2 h. Cells were fixed and stained as described above. The following concentrations were employed for treatment: for proteinase K, 8 μg/ml; for elastase, 2 mg/ml; for thermolysin, 200 μg/ml; for dispase, 1 unit/ml; for papain, 0.19 unit/ml; for chymotrypsin, 2 mg/ml; and for collagenase, 1 mg/ml. Protease (−) indicates the absence of protease.

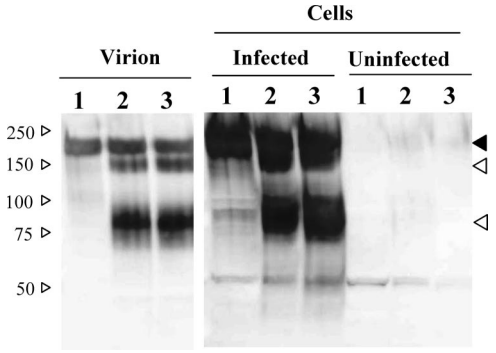

FIG. 2. Western blotting analysis of the 229E S protein after treatment with trypsin. (Left) 229E virions concentrated as described in Materials and Methods were treated with trypsin (lane 1, 0 μg/ml; lane 2, 50 μg/ml; lane 3, 100 μg/ml) at RT for 5 min. (Right) Also, 229E-infected and mock-infected HeLa cells were treated with trypsin (lanes 1, 0 μg/ml; lanes 2, 250 μg/ml; lanes 3, 500 μg/ml). The resultant samples were analyzed by Western blotting using anti-229E S antibodies raised with a synthetic peptide corresponding to the C-terminal region of the S protein. Uncleaved S protein and cleaved S2 protein are indicated by black and white arrowheads, respectively.

Effects of lysosomotropic agents on infection with 229E. As 229E produced syncytium formation in the presence of trypsin, which induces the cleavage of its S protein, and as 229E is similar to SARS-CoV and MHV-2, which take an endosomal pathway for infection, we deduced that 229E enters into cells in a fashion similar to that seen for those coronaviruses. To test this possibility, we examined the effects on 229E infection of the lysosomotropic agents Baf and NH_4Cl, known to prevent the acidification of the endosome and block infection via an endosomal pathway. First of all, we examined whether Baf treatment in an early phase of infection prevents infection or not. HeLa cells were continuously treated with Baf from 1 h before 229E infection to 4 h after infection, and the cells were cultured in the absence of Baf thereafter. Alternatively, cells were treated with Baf from 4 h to 24 h after infection. Virus titers in the culture at 24 h after infection were monitored. As shown in Fig. 4A, 229E infection was heavily (by ca. 1,000-fold) inhibited when cells were treated at −1 to 4 h of infection, while it was not so greatly influenced when cells were treated from 4 h after infection, which suggested to us that Baf treat-

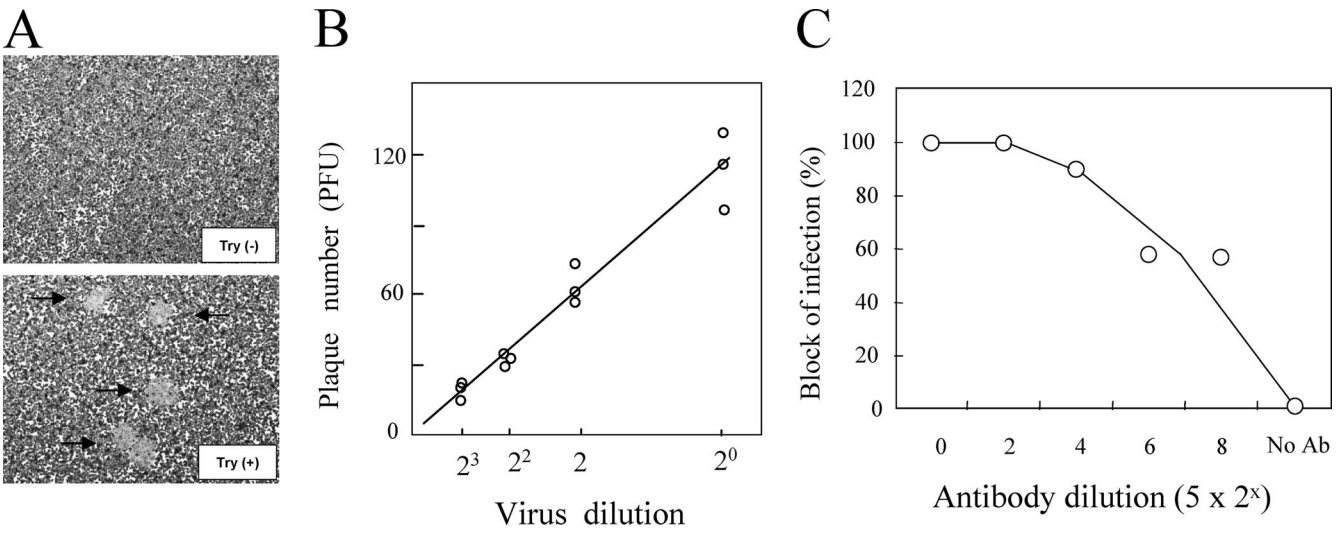

FIG. 3. Characterization of HeLa cells permissive for 229E infection. (A) HeLa cells infected with 229E and cultured for 1 day in the presence or absence of trypsin (Try; 5 μg/ml) in DMEM containing 10% TPB were fixed and stained as described above. The syncytia formed, indicated by arrows, were observed under microscopy as plaques. (B) To evaluate the plaque assay developed using HeLa cells and trypsin, 229E virion solutions at ca. 120 PFU/50 μl were diluted by twofold steps and inoculated into 3 wells of HeLa cells prepared in 24-well plates. The relationship between the virus dilution and the plaque number is depicted. (C) HeLa cells prepared in 96-well plates were treated with anti-human APN sera at 4°C for 45 min and then allowed to be adsorbed with ca. 150 PFU of 229E at 4°C for 45 min in the presence of antiserum. Next, those cells were cultured for 1 day in the presence of the antiserum. The infected cells were counted under fluorescence microscopy after cells had been stained with antibody (Ab) against 229E and secondary fluorescein isothiocyanate-labeled anti-rabbit serum. Cells in which infection was blocked by APN antibody were compared to those without APN antibody treatment.

ment impaired an early phase of 229E infection but not the phase later than 4 h. This finding could indicate that 229E takes an endosomal pathway and that the acidic conditions of endosomes are critical for its cell entry. We also examined the effects of Baf and NH_4Cl on the infection by 229E of HeLa-AC cells under the control of MHV-2, which requires acidic endosomal conditions for cell entry, and also of JHMV, which enters cells directly from the cell surface. As shown in Fig. 4B, the infection with MHV-2 was extensively suppressed by treatment with Baf and NH_4Cl, yet JHMV infection was hardly influenced, as expected due to the entry mechanisms of these two viruses that were shown by previous reports (16, 30). 229E infection in those cells was suppressed more efficiently than was that of MHV-2 by both of those agents, a finding leading us to suggest that 229E takes an endosomal pathway and that the acidic conditions of the endosomes are necessary for its infection. Furthermore, we have confirmed these observations by using pseudotyped VSV harboring the 229E S protein. VSV pseudotypes carrying SARS-CoV S protein or VSV glycoprotein were used as control viruses that take an endosomal pathway. HeLa-A cells treated with either Baf or NH_4Cl were infected with those pseudotypes, and infection was monitored by GFP expression at 24 h of infection. As shown in Fig. 4C, the infection with all of three pseudotypes was suppressed in an agent-concentration-dependent fashion. This result strengthened the observation above that 229E enters into cells via the endosomes of the acidic environment, in a manner similar to that seen for the infection with SARS-CoV and VSV.

Effects of protease inhibitors on infection with 229E. The above data led us to the possibility that 229E takes an endosomal pathway and that the acidic condition of the endosomes is necessary for its infection, although we could not clarify whether this virus requires proteases active in the endosome, as revealed with SARS-CoV, or whether a low-pH environment is sufficient for its infection, as shown by VSV; infection with the former but not the latter is blocked by protease inhibitors. To address this issue, cells treated with a variety of protease inhibitors were infected with pseudotypes bearing 229E S, SARS-CoV S, or VSV G, and their infection levels were estimated using GFP expression. As shown in Fig. 5, infection with the 229E pseudotype and that of SARS-CoV was prevented in a concentration-dependent manner by treatment with leupeptin (cysteine protease and trypsin-like protease inhibitor), MDL28107, and EST (both CPL inhibitors), as well as CPL inhibitor II, which implied that CPL is utilized by 229E for its infection. Infection by the pseudotype with 229E S protein was partially blocked by treatment with CPK inhibitor, but the inhibition was less prominent than that of the pseudotype with SARS-CoV S protein. Those pseudotypes were not drastically affected by treatment with CA-074 (CPB inhibitor). In contrast, the infection by the VSV G pseudotype was affected by none of those protease inhibitors. CPS inhibitor displayed an inhibitory effect for all of those pseudotype infections, even for one with VSV G protein, which requires no proteases thus far reported, leading us to the suggestion that CPS is not involved in the infection with 229E and that the inhibitory effects may be due to the side effects of CPS inhibitor. These results collectively suggested that 229E enters the cell in a protease-dependent fashion similar to that of SARS-CoV and that CPL is the primary candidate for activation of 229E entry into cells.

Effect of CPL knockdown by siRNA. To determine the role of CPL in 229E infection more directly, we knocked down the

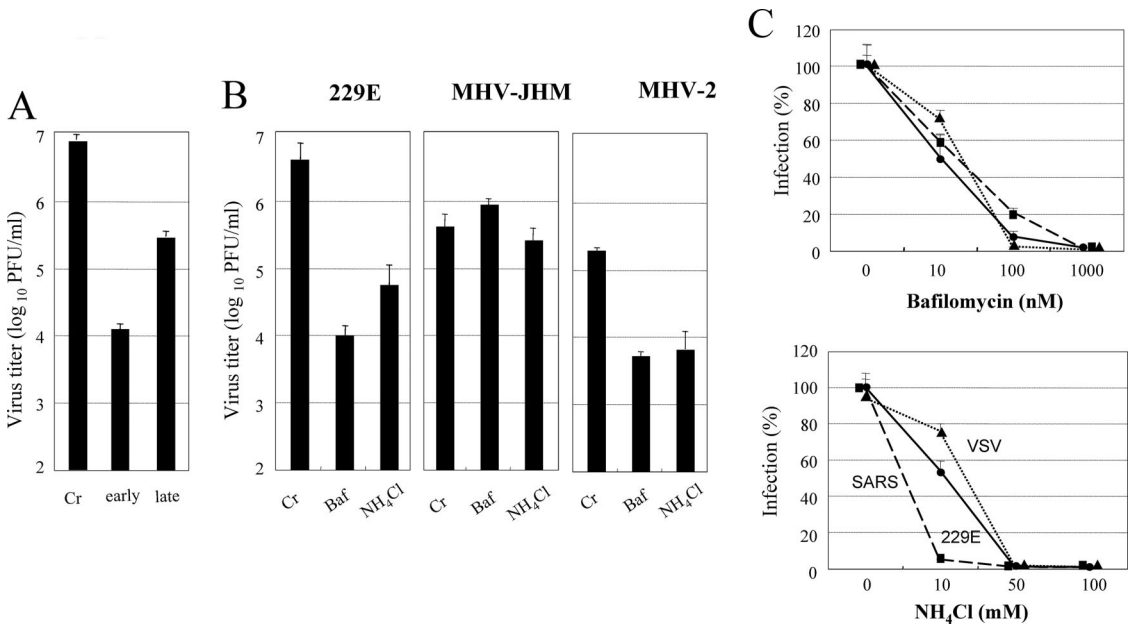

FIG. 4. Effect of lysosomotropic agents on 229E infection. (A) HeLa cells in 24-well plates were treated with 100 nM of Baf from 1 h before infection to 4 h postinfection (early) or from 4 to 24 h after 229E infection (late). Virus titers were determined for cells at 24 h postinfection. HeLa cells were infected at an MOI of 1. (B) HeLa-AC cells prepared in 24-well plates were treated with 1,000 nM of Baf or 50 mM NH_4Cl for 1 h at 37°C. Then, cells were infected with 1×10^5 PFU of virus (229E, MHV-JHM, or MHV-2) in DMEM containing each agent and incubated at 34°C (229E) or 37°C (MHV) for 1 h. After being washed once, cells were cultured with DMEM containing each agent for 3 h, and then medium was changed to DMEM without agent. Virus titers were examined by plaque assay in cells at 24 h (229E) or 10 h (MHV) after infection. (C) HeLa-A cells prepared in 96-well plates were treated with different concentrations of Baf or NH_4Cl for 1 h; infected with ca. 500 IU of pseudotyped VSV bearing 229E S (solid line with circle), SARS-CoV S (broken line with square), or VSV G protein (dotted line with triangle); and cultured for 24 h in the presence of each agent. Then, GFP-positive cells were photographed by Keyence fluorescence microscopy and counted. The percentage of infection was calculated as follows: (GFP-positive cell number in the presence of agent)/(GFP-positive cell number in the absence of agent) × 100. Cr, control.

CPL expression by siRNA as described in Materials and Methods. Cells treated with siRNA for 3 to 4 days were examined for CPL expression. As shown in Fig. 6A, CPL expression in cells treated with CPL siRNA, but not with control RNA, was reduced, as determined by examination with Western blotting. These cells were infected with a pseudotype bearing 229E S, SARS-CoV S, or VSV G, and their infection was monitored by GFP expression. As shown in Fig. 6B, infection with SARS-CoV pseudotype was blocked by ca. 80%, while a VSV G pseudotype was not at all blocked, a finding similar to the observations obtained from the protease inhibitor experiments. The infection with a 229E pseudotype was also blocked by the treatment with siRNA, yet it was not so drastically blocked as the infection with a SARS-CoV pseudotype. We consistently observed a reduction in infection of about 20 to 45%, which suggested to us that although CPL is involved in the infection initiated by 229E, some other proteases could also participate in the infection process.

Cleavage of virion S protein by CPL. Since protease inhibitors and siRNA analysis suggested that CPL is the most probable protease to induce the cleavage and fusion activation of 229E S protein, we have treated 229E virion S protein with CPL and analyzed the resultant S protein by Western blotting. As shown in Fig. 6C, 229E S protein was cleaved, resulting in the appearance of a fragment of ca. 100 kDa, while the cleavage was not found following the treatment with CPB. This suggested that 229E S protein is cleaved and activated for fusion by CPL. We have also treated virions with trypsin and compared the cleavage products of CPL and trypsin. As shown in Fig. 6C, the cleavage product of CPL, which was ca. 100 kDa, was slightly larger than that of trypsin, which was ca. 80 kDa. We also treated 229E-infected cells with CPL to see whether CPL induced cell-to-cell fusion, as revealed by Bosch et al. for SARS-CoV-infected cells (4), but it failed to induce cell-to-cell fusion (data not shown), although treatment with trypsin did induce fusion, as seen in Fig. 1.

Potentiation of 229E infection from the cell surface. The results described above indicate that 229E takes an endosomal pathway for cell entry and that the CPL and some other proteases that are active under a low-pH environment are critical for the fusogenic activation of the S protein. We then examined whether 229E is facilitated to enter cells from the cell surface, when receptor-bound 229E is treated with trypsin, which activates S protein fusion activity. This phenomenon was observed for SARS-CoV and MHV-2 infections (26, 30, 33). HeLa-A cells treated with Baf, an inhibitor of endosomal infection, were adsorbed with pseudotyped VSV bearing either 229E S, SARS-CoV S, or VSV G at 4°C for 30 min and then treated with trypsin. Infection with those pseudotypes was monitored by the expression of GFP. As shown in Fig. 7, infection by pseudotypes with 229E S as well as with SARS-CoV S was blocked by the Baf (Baf-positive, Try-negative) treatment, but the infection was facilitated when cell-adsorbed viruses were treated with trypsin (Baf positive, Try positive), while that with VSV G failed to infect even with trypsin treatment (Baf positive, Try positive). These results indicate that

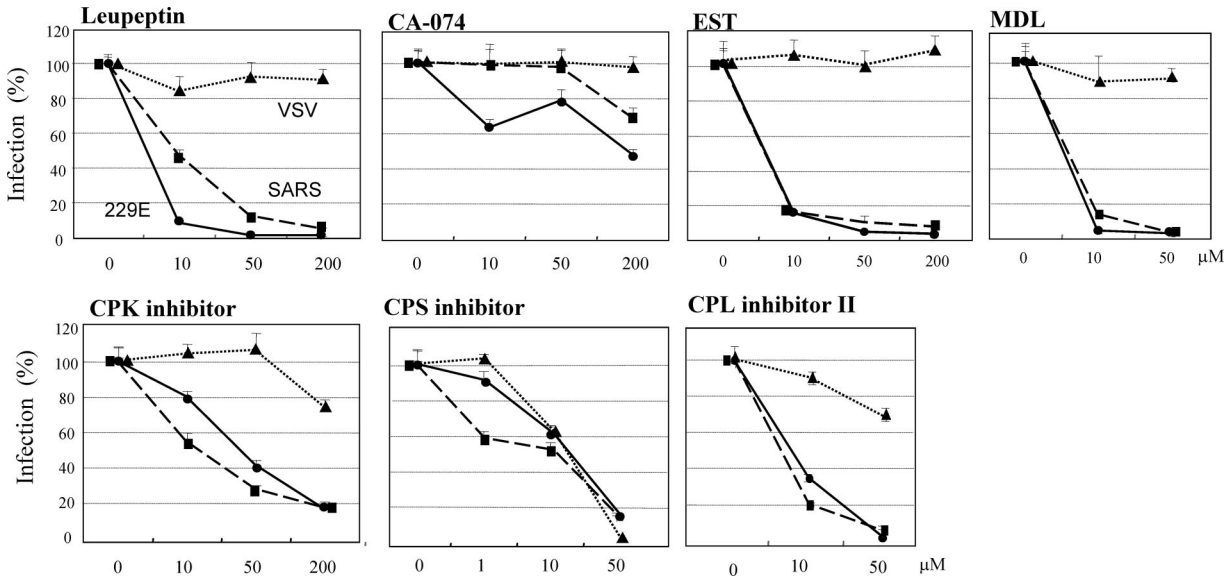

FIG. 5. Effects of protease inhibitors on pseudotyped virus infection. HeLa-A cells pretreated with different concentrations of protease inhibitors for 1 h were infected with ca. 500 IU of pseudotyped VSV bearing 229E S (solid line with circle); SARS-CoV S (broken line with square) or VSV G protein (dotted line with triangle) and cultured at 37°C for 24 h in the presence of protease inhibitors. The percentage of infection was determined as described for Fig. 4C. MDL, MDL28107.

viruses with 229E S as well as SARS-CoV S proteins enter cells from the cell surface in the presence of trypsin, while that with VSV G fails to do so. These results suggested that 229E enters cells directly from cell surface in the presence of protease, which activates fusion potential of 229E S protein.

DISCUSSION

In the present study, we have employed a few different approaches to analyze the 229E cell entry mechanism. We used infectious 229E together with the control viruses MHV-2 and JHMV; the former takes an endosomal pathway in a protease-dependent fashion, and the latter enters cells directly from a plasma membrane (16, 30). We also took advantage of VSV pseudotypes bearing 229E S together with those bearing SARS-CoV S protein and VSV G protein. SARS-CoV enters in a protease-dependent fashion and VSV in a pH-dependent fashion, although those two viruses enter from an endosomal compartment of acidic environment. To compare the cell entry features of 229E with those viruses, we established a cell line that expresses the receptors for SARS-CoV and MHV by use of HeLa cells originally permissive for 229E and VSV. By using these viruses, pseudotypes, and cells, we showed that 229E

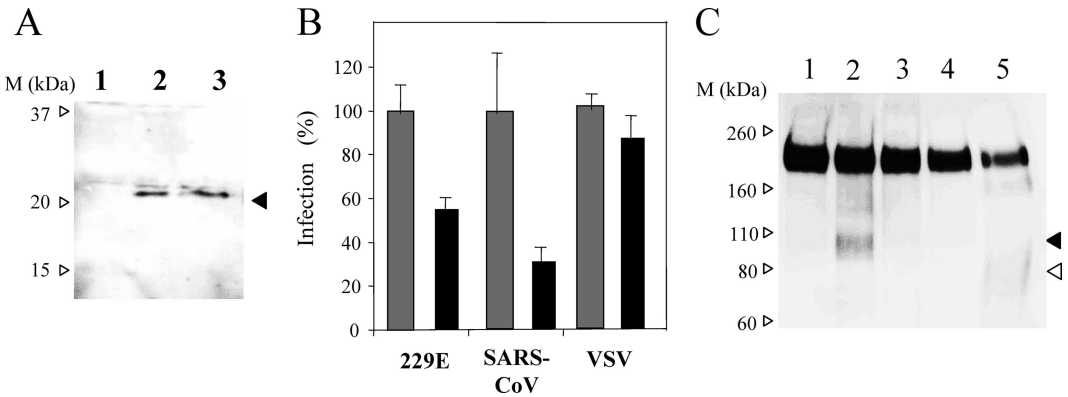

FIG. 6. Effect of CPL knockdown by siRNA on pseudotype infection (A and B) and digestion of 229E S by CPL (C). (A) HeLa-A cells were treated with siRNA for CPL (lane 1) and control nonsense RNA (lane 2) or were left untreated (lane 3) and cultured for 4 days. Amounts of CPL expressed in those cells were examined by Western blotting. The arrowhead indicates the position of CPL. (B) HeLa-A cells transfected with CPL siRNA and cultured for 4 days (black columns) were infected with ca. 500 IU of pseudotyped VSV with 229E S, SARS-CoV S, or VSV G protein. Their infection rates (GFP-positive cell numbers) were compared to those for cells transfected with control RNA (gray columns). (C) 229E virions concentrated as described in Materials and Methods were treated with 36 μg/ml of CPL (lane 2) or CPB (lane 3) or were mock treated (lane 1) at 37°C for 30 min in a buffer at pH 5.0, and S protein was analyzed by Western blotting using anti-229E S antibodies as described in the Fig. 2 legend. As a control, virions were also treated (lane 5) or mock treated (lane 4) with 50 μg/ml of trypsin at 37°C for 30 min in a buffer at pH. 70 and analyzed by Western blotting. M, molecular mass.

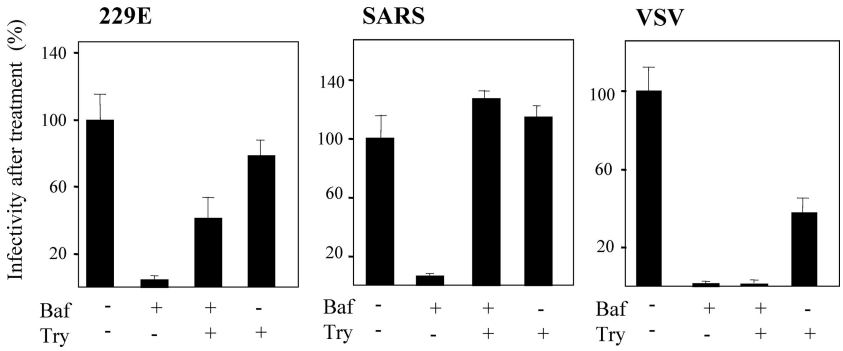

FIG. 7. Infection with 229E S-bearing pseudotyped VSV from cell surfaces. HeLa-A cells prepared in 96-well plates were treated with 100 nM Baf for 1 h at 37°C and then allowed to adsorb VSV bearing 229E S, SARS-CoV S, or VSV G protein on ice for 30 min. The plate was left at RT for 10 min, and adsorbed virus was treated with 100 μg/ml trypsin for 5 min. Then, those cells were cultured for 24 h at 37°C, and GFP-positive cell numbers were calculated as described above (Baf positive, Try positive). GFP-positive cell numbers were also determined for the groups of cells treated with Baf alone (Baf +, Try −) or trypsin alone (Baf −, Try +) or maintained as untreated control cells (Baf −, Try −). The number of GFP-positive cells in each group is shown as a percentage in comparison with that of GFP-positive cells without any treatment.

enters cells by endocytosis and that proteases active at low-pH condition are critical for its infection. CPL is a possible protease that enables the fusogenic activation of the 229E S protein; however, some other not-yet-identified proteases active under a low-pH environment and also sensitive to cysteine protease inhibitor could be involved in this activation. Thus, 229E is the third coronavirus (and the first group 1 coronavirus) shown to enter cells in a protease-dependent fashion. The uncleavability of 229E S protein is shared by the group 2 coronaviruses SARS-CoV and MHV-2 as well as most members of group 1, including transmissible gastroenteritis virus, feline infectious peritonitis virus, and the like (6). It is of interest to see whether those group 1 coronaviruses also utilize a protease-dependent entry like that of 229E.

The entry pathway of 229E has not been adequately studied, although the interaction of its receptor and S protein has been well investigated (3, 41). Nomura et al. reported that 229E enters cells in a caveolin-mediated fashion (28). They showed that caveolin-1 and 229E receptor APN colocalized on the lipid raft on the cell membrane and that inoculated 229E colocalized with caveolin-1. In addition to the binding of 229E to ANP molecules associated with the caveolin-1 molecule, they further showed that the knockdown of caveolin-1 by siRNA reduced the infection with 229E, albeit the reduction was moderate (28). In contrast, our data shown in this study revealed that the blockade of the endosomal pathway, e.g., by treatment with Baf and NH_4Cl, reduced the infection quite efficiently, by 2 orders of magnitude. Generally, viruses that are endocytosed via caveolae are targeted to the endoplasmic reticulum or Golgi and not to the endosome (32). However, it could happen that 229E incorporated into caveolae is trafficked to the endosome, although it is not a general pathway of caveolin-mediated infection or caveolin-mediated endocytosis. A detailed study of the 229E entry pathway could delineate a new mechanism of viral invasion into the cell.

The fusion activity of the coronavirus S proteins is thought to be independent of the cleavage site of the S protein. SARS-CoV S protein is fusogenically activated when cleaved at amino acid position 667 by trypsin and also at 678 by CPL (4, 22). We recently observed that SARS-CoV S protein cleaved at position 798, a position ca. 120 amino acids downstream of the cleavage sites of trypsin and CPL, is also fusogenic (43). As shown in this study, 229E S protein can be activated for the fusion of envelopes and cell membranes, even if the protein is cleaved in a different position in the S protein. Judging from the sizes of cleavage products, namely, ca. 100 kDa and 80 kDa by CPL and trypsin treatment, respectively, the CPL cleavage site would be around the putative S1-S2 junction region (amino acid 576 from an initiator of S), which was assumed by the sequence alignment of various coronavirus S proteins (14), while that of trypsin is located further downstream. Since the fusion peptide on coronavirus S protein is not located at the N terminus of the membrane-anchored subunit, different from what is the case for the envelope proteins of HIV or influenza virus, multiple forms of the S2 subunit could be functional in virus-cell fusion if the fusion peptide is located at a position accessible to the target membrane. Analysis of the precise cleavage site and fusion peptide of the 229E S protein will delineate the mechanism of how S2 interacts with the target membranes.

It should be noted that three different modes of cell entry are utilized by various coronaviruses; one from the plasma membrane and the others from an endosomal membrane in a low-pH-dependent or a protease-dependent fashion. The MHV-JHMV strain is thought to enter cells from the cell surface, since its infection results in an extensive cell-to-cell fusion in a wide range of pHs and is not influenced by the treatment of cells with lysosomotropic agents (16). In contrast, SARS-CoV enters cells via an endosomal compartment in a low-pH environment (26, 34). SARS-CoV S protein is activated by a protease (protease-dependent entry), such as CPL, in the endosome (4, 18, 33). Endosomal conditions of acidity are critical for protease activation, which induces cleavage of the SARS-CoV S protein. Previous and present studies on MHV-2 (30) and 229E, respectively, showed that those utilize a mechanism for cell entry similar to that of SARS-CoV. On the other hand, a mutant MHV isolated from persistently infected cells was reported to utilize an endosomal pathway similar to that of the influenza virus' low-pH-dependent entry (16). Quite recently, avian infectious bronchitis virus and MHV-A59 also have been reported to utilize a similar entry mode; moreover, the S proteins of those viruses are fusogeni-

cally activated under a low-pH environment, and no protease is required for activation (9, 13), although the entry mechanism of MHV-A59 is still controversial, since entry from cell surface and other mechanisms of fusion activation have been reported (29, 30, 52). These observations indicate that coronavirus S protein is an appropriate tool to study the viral entry mechanism in terms of its molecular aspects.

Three different coronaviruses, SARS-CoV, MHV-2, and 229E, have been shown to enter cells directly from the cell surface, when the virion S proteins adsorbed to the cell surface receptor are cleaved with proteases such as trypsin that activate the fusion activity of those S proteins. In agreement with those findings, the cleaved S protein of SARS-CoV was recently shown to mediate the infection from the cell surface (43). In SARS-CoV infection, cell surface entry seemed to be more efficient than entry via the endosomes (26), which could account for the extraordinarily high replication in the lungs, where elastase, a protease to enable SARS-CoV entry from the cell surface (26), is secreted during the development of mild pneumonia. This efficient infection in the lungs could be a trigger for SARS, which was reproduced recently in mice infected with SARS-CoV and respiratory bacteria (1). Although 229E fails to induce a serious respiratory disease in humans, selective infection in the upper respiratory tract could be attributed to the specific proteases that could enable 229E infection from the cell surface. Since the 229E receptor APN is expressed in a wide variety of cells in the body (17), and 229E infection is limited in the upper respiratory tract, a host factor other than the receptor that determines the tissue specificity of 229E must exist. Protease, which enhances the infection, as observed for SARS-CoV infection (1, 26), may also participate in the pathogenesis of 229E infection. To delineate the pathogenesis of 229E, an analysis of such proteases would be an important direction.

ACKNOWLEDGMENTS

We thank Naoko Matsubara for her technical assistance and Shigeru Morikawa for his valuable suggestions on the use of HeLa cells for 229E infection. We also thank Ryuji Nomura for 229E and anti-229E S serum and M. A. Whitt for the VSV pseudotype system.

This work was financially supported by grants-in-aid from the Ministry of Education, Culture, Sports, Science and Technology of Japan (grant no. 19390135 and no. 19041073).

REFERENCES

1. **Ami, Y., N. Nagata, K. Shirato, R. Watanabe, N. Iwata, K. Nakagaki, S. Fukushi, M. Saijo, S. Morikawa, and F. Taguchi.** 2008. Co-infection of respiratory bacterium with severe acute respiratory syndrome coronavirus induces an exacerbated pneumonia in mice. Microbiol. Immunol. **52:**118–127.
2. **Appleyard, G., and M. Tisdale.** 1985. Inhibition of the growth of human coronavirus 229E by leupeptin. J. Gen. Virol. **66:**363–366.
3. **Bonavia, A., B. D. Zelus, D. E. Wentworth, P. J. Talbot, and K. V. Holmes.** 2003. Identification of a receptor-binding domain of the spike glycoprotein of human coronavirus HCoV-229E. J. Virol. **77:**2530–2538.
4. **Bosch, B. J., W. Bartelink, and P. J. Rottier.** 2008. Cathepsin L functionally cleaves the severe acute respiratory syndrome coronavirus class I fusion protein upstream of rather than adjacent to the fusion peptide. J. Virol. **82:**8887–8890.
5. **Bosch, B. J., B. E. Martina, R. Van Der Zee, J. Lepault, B. J. Haijema, C. Versluis, A. J. Heck, R. De Groot, A. D. Osterhaus, and P. J. Rottier.** 2004. Severe acute respiratory syndrome coronavirus (SARS-CoV) infection inhibition using spike protein heptad repeat-derived peptides. Proc. Natl. Acad. Sci. USA **101:**8455–8460.
6. **Cavanagh, D.** 1995. The coronavirus surface glycoprotein, p. 73–113. *In* S. G. Siddell (ed.), The Coronaviridae. Plenum Press, New York, NY.
7. **Chan, D. C., and P. S. Kim.** 1998. HIV entry and its inhibition. Cell **93:**681–684.
8. **Chandran, K., N. J. Sullivan, U. Felbor, S. P. Whelan, and J. M. Cunningham.** 2005. Endosomal proteolysis of the Ebola virus glycoprotein is necessary for infection. Science **308:**1643–1645.
9. **Chu, V. C., L. J. McElroy, V. Chu, B. E. Bauman, and G. R. Whittaker.** 2006. The avian coronavirus infectious bronchitis virus undergoes direct low-pH-dependent fusion activation during entry into host cells. J. Virol. **80:**3180–3188.
10. **Dveksler, G. S., M. N. Pensiero, C. B. Cardellichio, R. K. Williams, G. S. Jiang, K. V. Holmes, and C. W. Dieffenbach.** 1991. Cloning of the mouse hepatitis virus (MHV) receptor: expression in human and hamster cell lines confers susceptibility to MHV. J. Virol. **65:**6881–6891.
11. **Dveksler, G. S., M. N. Pensiero, C. W. Dieffenbach, C. B. Cardellichio, A. A. Basile, P. E. Elia, and K. V. Holmes.** 1993. Mouse hepatitis virus strain A59 and blocking antireceptor monoclonal antibody bind to the N-terminal domain of cellular receptor. Proc. Natl. Acad. Sci. USA **90:**1716–1720.
12. **Eckert, D. M., and P. S. Kim.** 2001. Mechanisms of viral membrane fusion and its inhibition. Annu. Rev. Biochem. **70:**777–810.
13. **Eifart, P., K. Ludwig, C. Bottcher, C. A. de Haan, P. J. Rottier, T. Korte, and A. Herrmann.** 2007. Role of endocytosis and low pH in murine hepatitis virus strain A59 cell entry. J. Virol. **81:**10758–10768.
14. **Follis, K. E., J. York, and J. H. Nunberg.** 2006. Furin cleavage of the SARS coronavirus spike glycoprotein enhances cell-cell fusion but does not affect virion entry. Virology **350:**358–369.
15. **Fukushi, S., T. Mizutani, M. Saijo, S. Matsuyama, N. Miyajima, F. Taguchi, S. Itamura, I. Kurane, and S. Morikawa.** 2005. Vesicular stomatitis virus pseudotyped with severe acute respiratory syndrome coronavirus spike protein. J. Gen. Virol. **86:**2269–2274.
16. **Gallagher, T. M., C. Escarmis, and M. J. Buchmeier.** 1991. Alteration of the pH dependence of coronavirus-induced cell fusion: effect of mutations in the spike glycoprotein. J. Virol. **65:**1916–1928.
17. **Holmes, K. V., and S. R. Compton.** 1995. Coronavirus receptors, p. 55–71. *In* S. G. Siddell (ed.), The Coronaviridae. Plenum Press, New York, NY.
18. **Huang, I. C., B. J. Bosch, F. Li, W. Li, K. H. Lee, S. Ghiran, N. Vasilieva, T. S. Dermody, S. C. Harrison, P. R. Dormitzer, M. Farzan, P. J. Rottier, and H. Choe.** 2006. SARS coronavirus, but not human coronavirus NL63, utilizes cathepsin L to infect ACE2-expressing cells. J. Biol. Chem. **281:**3198–3203.
19. **Kubo, H., S. Takase-Yoden, and F. Taguchi.** 1993. Neutralization and fusion inhibition activities of monoclonal antibodies specific for the S1 subunit of the spike protein of neurovirulent murine coronavirus JHMV c1-2 variant. J. Gen. Virol. **74:**1421–1425.
20. **Kusanagi, K., H. Kuwahara, T. Katoh, T. Nunoya, Y. Ishikawa, T. Samejima, and M. Tajima.** 1992. Isolation and serial propagation of porcine epidemic diarrhea virus in cell cultures and partial characterization of the isolate. J. Vet. Med. Sci. **54:**313–318.
21. **Lai, M. M., and D. Cavanagh.** 1997. The molecular biology of coronaviruses. Adv. Virus Res. **48:**1–100.
22. **Li, F., M. Berardi, W. Li, M. Farzan, P. R. Dormitzer, and S. C. Harrison.** 2006. Conformational states of the severe acute respiratory syndrome coronavirus spike protein ectodomain. J. Virol. **80:**6794–6800.J.
23. **Li, W., M. J. Moore, N. Vasilieva, J. Sui, S. K. Wong, M. A. Berne, M. Somasundaran, J. L. Sullivan, K. Luzuriaga, T. C. Greenough, H. Choe, and M. Farzan.** 2003. Angiotensin-converting enzyme 2 is a functional receptor for the SARS coronavirus. Nature **426:**450–454.
24. **Matsuyama, S., and F. Taguchi.** 2000. Impaired entry of soluble receptor-resistant mutants of mouse hepatitis virus into cells expressing MHVR2 receptor. Virology **273:**80–89.
25. **Matsuyama, S., and F. Taguchi.** 2002. Receptor-induced conformational changes of murine coronavirus spike protein. J. Virol. **76:**11819–11826.
26. **Matsuyama, S., M. Ujike, S. Morikawa, M. Tashiro, and F. Taguchi.** 2005. Protease-mediated enhancement of severe acute respiratory syndrome coronavirus infection. Proc. Natl. Acad. Sci. USA **102:**12543–12547.
27. **Miura, H. S., K. Nakagaki, and F. Taguchi.** 2004. N-terminal domain of the murine coronavirus receptor CEACAM1 is responsible for fusogenic activation and conformational changes of the spike protein. J. Virol. **78:**216–223.
28. **Nomura, R., A. Kiyota, E. Suzaki, K. Kataoka, Y. Ohe, K. Miyamoto, T. Senda, and T. Fujimoto.** 2004. Human coronavirus 229E binds to CD13 in rafts and enters the cell through caveolae. J. Virol. **78:**8701–8708.
29. **Pu, Y., and X. Zhang.** 2008. Mouse hepatitis virus type 2 enters cells through a clathrin-mediated endocytic pathway independent of Eps15. J. Virol. **82:**8112–8123.
30. **Qiu, Z., S. T. Hingley, G. Simmons, C. Yu, J. Das Sarma, P. Bates, and S. R. Weiss.** 2006. Endosomal proteolysis by cathepsins is necessary for murine coronavirus mouse hepatitis virus type 2 spike-mediated entry. J. Virol. **80:**5768–5776.
31. **Saeki, K., N. Ohtsuka, and F. Taguchi.** 1997. Identification of spike protein residues of murine coronavirus responsible for receptor-binding activity by use of soluble receptor-resistant mutants. J. Virol. **71:**9024–9031.
32. **Sieczkarski, S. B., and G. R. Whittaker.** 2005. Viral entry. Curr. Top. Microbiol. Immunol. **285:**1–23.
33. **Simmons, G., D. N. Gosalia, A. J. Rennekamp, J. D. Reeves, S. L. Diamond, and P. Bates.** 2005. Inhibitors of cathepsin L prevent severe acute respiratory syndrome coronavirus entry. Proc. Natl. Acad. Sci. USA **102:**11876–11881.

34. **Simmons, G., J. D. Reeves, A. J. Rennekamp, S. M. Amberg, A. J. Piefer, and P. Bates.** 2004. Characterization of severe acute respiratory syndrome-associated coronavirus (SARS-CoV) spike glycoprotein-mediated viral entry. Proc. Natl. Acad. Sci. USA **101:**4240–4245.
35. **Sturman, L. S., C. S. Ricard, and K. V. Holmes.** 1985. Proteolytic cleavage of the E2 glycoprotein of murine coronavirus: activation of cell-fusing activity of virions by trypsin and separation of two different 90K cleavage fragments. J. Virol. **56:**904–911.
36. **Suzuki, H., and F. Taguchi.** 1996. Analysis of the receptor-binding site of murine coronavirus spike protein. J. Virol. **70:**2632–2636.
37. **Taguchi, F., and S. Matsuyama.** 2002. Soluble receptor potentiates receptor-independent infection by murine coronavirus. J. Virol. **76:**950–958.
38. **Taguchi, F., S. G. Siddell, H. Wege, and V. ter Meulen.** 1985. Characterization of a variant virus selected in rat brains after infection by coronavirus mouse hepatitis virus JHM. J. Virol. **54:**429–435.
39. **Takada, A., C. Robison, H. Goto, A. Sanchez, K. G. Murti, M. A. Whitt, and Y. Kawaoka.** 1997. A system for functional analysis of Ebola virus glycoprotein. Proc. Natl. Acad. Sci. USA **94:**14764–14769.
40. **Toth, T. E.** 1982. Trypsin-enhanced replication of neonatal calf diarrhea coronavirus in bovine embryonic lung cells. Am. J. Vet. Res. **43:**967–972.
41. **Tusell, S. M., S. A. Schittone, and K. V. Holmes.** 2007. Mutational analysis of aminopeptidase N, a receptor for several group 1 coronaviruses, identifies key determinants of viral host range. J. Virol. **81:**1261–1273.
42. **Ujike, M., H. Nishikawa, A. Otaka, N. Yamamoto, M. Matsuoka, E. Kodama, N. Fujii, and F. Taguchi.** 2008. Heptad repeat-derived peptides block protease-mediated direct entry from the cell surface of severe acute respiratory syndrome coronavirus but not entry via the endosomal pathway. J. Virol. **82:**588–592.
43. **Watanabe, R., S. Matsuyama, K. Shirato, M. Maejima, S. Fukushi, S. Morikawa, and F. Taguchi.** 2008. Entry from cell surface of SARS coronavirus with cleaved S protein as revealed by pseudotype virus bearing cleaved S protein. J. Virol. **82:**11985–11991.
44. **Wege, H., S. Siddell, and V. ter Meulen.** 1982. The biology and pathogenesis of coronaviruses. Curr. Top. Microbiol. Immunol. **99:**165–200.
45. **White, J. M.** 1990. Viral and cellular membrane fusion proteins. Annu. Rev. Physiol. **52:**675–697.
46. **Williams, R. K., G. S. Jiang, and K. V. Holmes.** 1991. Receptor for mouse hepatitis virus is a member of the carcinoembryonic antigen family of glycoproteins. Proc. Natl. Acad. Sci. USA **88:**5533–5536.
47. **Wool-Lewis, R. J., and P. Bates.** 1998. Characterization of Ebola virus entry by using pseudotyped viruses: identification of receptor-deficient cell lines. J. Virol. **72:**3155–3160.
48. **Yamada, Y. K., K. Takimoto, M. Yabe, and F. Taguchi.** 1997. Acquired fusion activity of a murine coronavirus MHV-2 variant with mutations in the proteolytic cleavage site and the signal sequence of the S protein. Virology **227:**215–219.
49. **Yeager, C. L., R. A. Ashmun, R. K. Williams, C. B. Cardellichio, L. H. Shapiro, A. T. Look, and K. V. Holmes.** 1992. Human aminopeptidase N is a receptor for human coronavirus 229E. Nature **357:**420–422.
50. **Yoshikura, H., and S. Tejima.** 1981. Role of protease in mouse hepatitis virus-induced cell fusion. Studies with a cold-sensitive mutant isolated from a persistent infection. Virology **113:**503–511.
51. **Zamoto, A., F. Taguchi, S. Fukushi, S. Morikawa, and Y. K. Yamada.** 2006. Identification of ferret ACE2 and its receptor function for SARS-coronavirus. Adv. Exp. Med. Biol. **581:**519–522.
52. **Zelus, B. D., J. H. Schickli, D. M. Blau, S. R. Weiss, and K. V. Holmes.** 2003. Conformational changes in the spike glycoprotein of murine coronavirus are induced at 37°C either by soluble murine CEACAM1 receptors or by pH 8. J. Virol. **77:**830–840.